All about Nitrite: Exploring Nitrite Sources and Sinks in Oxygen Minimum Zones

Supplementary Materials

John C. Tracey[1, 2], Andrew R. Babbin[3], Elizabeth Wallace[1], Xin Sun[1, 4], Katherine L. DuRussel[1, 5], Claudia Frey[1, 6], Donald E. Martocello III[3], Tyler Tamasi[3], Sergey Oleynik[1], and Bess B. Ward[1]

[1] Department of Geosciences, Princeton University, Guyot Hall, Princeton, NJ, USA 08544
[2] Department of Biology and Paleo Environment, Lamont Doherty Earth Observatory, Columbia University, Palisades, NY, USA 10964
[3] Department of Earth, Atmospheric and Planetary Sciences, Massachusetts Institute of Technology, Cambridge, MA, USA 02138
[4] Department of Global Ecology, Carnegie Institution for Science, Stanford, CA, USA 94305
[5] Department of Civil and Environmental Engineering, Northwestern University, Evanston, IL, USA 60208
[6] Department of Environmental Sciences, University of Basel, Bernoullistrasse 30, 4056 Basel, Switzerland

Correspondence to: John C. Tracey (jt16@alumni.princeton.edu)

Supplementary Material:

Additional Information on Anammox and Denitrification Profiles (SR1805 and FK180624)

In order to calculate the denitrification and anammox rates using Eq. $(7-9)$, the amount of 29 and 30 N_2 in nmol for each vial must first be calculated using the equations below:

$$29_{N_{2_{nmol}}} = (Slope_{STD\ Curve}) * \frac{29}{28}_{A_M} * \widehat{28}_{N_{2_{Peak\ Area}}} \tag{S1}$$

$$30_{N_{2_{nmol}}} = (Slope_{STD\ Curve}) * \frac{30}{28}_{A_M} * \widehat{28}_{N_{2_{Peak\ Area}}} \tag{S2}$$

Where:

$\frac{30}{28}_{A_M}$ or $\frac{29}{28}_{A_M}$ is the measured ratio in peak area units of the specific sample,

$\widehat{28}_{N_{2_{Peak\ Area}}}$ is the average 28 peak area across the time course (without outliers), and

$Slope_{STD\ Curve}$ is the standard curve slope in nmol / peak area units.

Outliers were defined as values more than three standard deviations away from the time course mean. The average 28 peak area across the time course was used as a data smoothing technique to remove variation due to small differences in the water volume aliquoted into each exetainer.

If necessary, drift corrections were performed as follows. First, the 29 / 28 and 30 / 28 ratios of the standards from each mass spectrometer (MS) run were regressed using both linear and logarithmic models against the total N of each sample. If the regressions returned slopes significantly different from zero via a Student's T test (p values <0.05), a drift correction was performed using the best regression (as determined by R^2 and the residual mean square error (RMSE) values). Corrections were performed by using the best significant regression to calculate a theoretical value for each total N point. After this the difference between an "endpoint" (the endpoint varied from run to run - the highest or lowest theoretical value for one of the standards was used) and each theoretical value was calculated for every point. This difference was then added to the raw sample and standard values to correct for drift. After performing total N drift corrections, corrected ratios were re-plotted against total N to examine if the correction was successful. After performing a total N correction, samples were examined for drift due to the time in the mass spectrometer run. This was performed in an analogous manner to the total N drift correction.

Drift corrected values were then used to calculate rates via Eq. (7 – 9). Importantly, the rates reported here were not all calculated using regressions from $t_0 - t_4$. Instead, regressions from $t_0 - t_2$, $t_0 - t_3$, and $t_0 - t_4$ were compared and the best regression was selected based on a combination of the R^2 and RMSE value. Rates due to a bottle effect (i.e., exponential growth of

an N cycling microbe at the end of the incubation because incubation conditions changed over the course of the experiment to favor exponential growth) were removed by comparing linear and exponential models for any suspected time courses. If the exponential model was a better fit, the rate from that time course was not reported and the next shorter significant time course ($t_0 - t_2$, or $t_0 - t_3$) for that incubation was used.

For the SR1805 cruise, anammox rates calculated from the $^{15}NH_4^+$ and $^{15}NO_2^-$ tracers were similar in magnitude (Supplementary Table S3). As a result, the SR1805 anammox rates reported in Figs. 2, 3, 6, 7, 8, and 9 represent either the average of the rates calculated from the $^{15}NH_4^+$ and $^{15}NO_2^-$ tracers (if significant rates were returned for both tracers) or the rate from the tracer that returned a significant or positive rate with error bars above zero. The FK180624 anammox rates reported in Fig. S1 are from the $^{15}NO_2^-$ tracer alone.

Additional Information for NO_2^- Oxidation Rate Measurements

Methods Details for Depth Profiles

The denitrifying bacterium culture seed (*Pseudomonas chloroaphis*) was prepared aerobically and frozen until needed. The denitrifiers were allowed to grow to high biomass for approximately five days so all NO_3^- in the growth medium was consumed. The denitrifiers were then concentrated through centrifugation and resuspended in a medium that lacked NO_3^-. The concentrate was distributed in 20 mL Grace vials (Manufacturer: Thermo Fisher Scientific, Bremen, Germany), sealed, and purged of O_2 with He for $3 - 5$ hours. Grace vials were chosen because their straight shape allows for minimum O_2 contamination while purging. After removing N_2, exetainers were prepared for the denitrifier method by subsampling 1 mL and then adding 30 µL sulfamic acid to consume any residual ambient or tracer NO_2^- present. After this,

30 µL of 5 N NaOH was added to return each sample to its original pH (Granger, J., & Sigman, 2009). The Grace vials were then injected with 1 mL of the sulfamic acid treated seawater samples and incubated overnight in the dark to convert NO_3^- to N_2O. Five to six drops of 10 N NaOH was added to terminate the reactions in the vials, and 5-6 drops of Antifoam B were added so the solution would not foam when purged with helium by the mass spectrometer. Drift corrections, mechanism for selecting the best time course from $t_0 - t_2$, $t_0 - t_3$, and $t_0 - t_4$, and checks for bottle effects were conducted in similar ways to those described above for anammox and denitrification depth profiles.

Method Details for Dismutation Experiments

Measurements of anammox, denitrification, and NO_2^- oxidation for the dismutation tests were conducted as above except for the following changes:

(1) For the $^{15}NO_3^-$ measurements of the dismutation experiments, 200 µL of acidified seawater sample was injected into each Grace vial instead of the 1 mL used in the depth profiles.

(2) For the anammox and denitrification measurements of the dismutation experiments, unlike in the depth profile experiments, each replicate within the 5 points of our 15 member time course was run on separate MS runs (i.e. $t_{0\ point\ 1}$, $t_{1\ point\ 1}$, $t_{2\ point\ 1}$, $t_{3\ point\ 1}$, and $t_{4\ point\ 1}$, were run together while $t_{0\ point\ 2}$, $t_{1\ point\ 2}$, $t_{2\ point\ 2}$, $t_{3\ point\ 2}$, and $t_{4\ point\ 2}$ and $t_{0\ point\ 3}$, $t_{1\ point\ 3}$, $t_{2\ point\ 3}$, $t_{3\ point\ 3}$, and $t_{4\ point\ 3}$ were run on separate runs. Samples were corrected for time and linearity in each separate MS run as in the depth profile experiments. After performing these corrections, the fifteen points from each time course were combined; however, the resulting time courses often had widely disparate ranges. In order to reduce the error of the rate regression, the range between mini time

courses (i.e., $t_{0 \text{ point 1}}$, $t_{1 \text{ point 1}}$, $t_{2 \text{ point 1}}$, $t_{3 \text{ point 1}}$, and $t_{4 \text{ point 1}}$ is one "mini" course out of three per depth), was condensed using the following method:

(a) Linear regressions for each of the mini time courses were calculated.

(b) Using these regressions, theoretical values at each point in the mini time courses were calculated.

(c) The average of these theoretical values for each of the three mini time courses was calculated.

(d) A linear regression for the whole time course was calculated.

(e) Using the whole time course regression, theoretical values at each of the five time points in the full length time course was calculated.

(f) The average of these five theoretical values was calculated.

(g) The difference between each mini time course's average and the full length average was calculated.

(h) This difference was added to each point in the run to condense the mini time courses' range.

The remaining calculations were performed as in the depth profile experiments.

Station	OMZ region	Bottom Z (m)	Coordinates	Depths (m)	Feature
PS1	Offshore	4100	10N	30	Oxic surface
			113W	60	Oxycline
				70	Oxycline
				90	ODZ top
				100	ODZ top
				110	ODZ top
				150	ODZ top
				260	ODZ core
				500	ODZ core
				1000	Oxycline
PS2	Open ocean	3000	15.76N	60	Oxic surface
			105W	75	Oxycline
				95	ODZ top
				120	ODZ top
				150	ODZ top
				200	ODZ top/SNM
				250	ODZ core/SNM
				300	ODZ core
				500	ODZ core
				850	ODZ core
PS3	Coastal	1030	17.68N	16	Oxycline
			102.35W	25	Oxycline
				35	Oxycline
				45	ODZ top
				60	ODZ top
				70	ODZ top
				100	ODZ top
				160	ODZ top/SNM
				250	ODZ core
				800	ODZ core

Supplementary Table S1: Sampling depths and geography for NH_4^+ oxidation, NO_3^- reduction, NO_2^- oxidation, anammox, and denitrification profiles (SR1805). Features are classified based on their potential density and O_2 concentrations. ODZ core samples have a $\sigma_\theta > 26.4$ (Babbin et al., 2020). ODZ top, oxycline, and oxic surface samples have a $\sigma_\theta < 26.4$ (Babbin et al., 2020).

Station	OMZ region	Bottom Z (m)	Coordinates	Depths (m)	Feature
2	Open ocean	3450	14N, 103W	102	Oxycline
				105	ODZ top
				120	ODZ top
				130	ODZ top
				200	ODZ top/SNM
				395	ODZ core
3	Open ocean	3000	14N, 104W	120	ODZ top
				140	ODZ top
				170	ODZ top
				250	ODZ core
9	Open ocean	3250	14N, 110W	96	Oxycline
				100	Oxycline
				105	ODZ top
				115	ODZ top
				130	ODZ top
				160	ODZ top/SNM
				168	ODZ core/SNM
				175	ODZ core/SNM
				200	ODZ core/SNM
				250	ODZ core/SNM
				300	ODZ core
				375	ODZ core
				475	ODZ core
				730	ODZ core
11	Open ocean	4000	14N, 112W	116	ODZ top
				320	ODZ core
12	Open ocean	4100	14N, 113W	103	ODZ top
				120	ODZ top
				150	ODZ top/SNM
				610	ODZ core
14	Open ocean	4100	14N, 115W	125	ODZ top/SNM
				323	ODZ core
15	Open ocean	4200	14N, 116W	135	ODZ top
				160	ODZ top
18	OMZ boundary	4100	17N, 119W	130	Oxycline
				160	Oxycline
				200	ODZ core

Supplementary Table S2: Sampling depths and geography for anammox, and denitrification profiles (FK180624). Features are classified based on their potential density and O_2 concentrations. ODZ core samples have a $\sigma_\theta > 26.4$ (Babbin et al., 2020). ODZ top, oxycline, and oxic surface samples have a $\sigma_\theta < 26.4$ (Babbin et al., 2020).

Depth (m)	Denitrification		Anammox ($^{15}NH_4^+$)		Anammox ($^{15}NO_2^-$)		Consensus anammox	
	Rate	Error	Rate	Error	Rate	Error	Rate	Error
PS1								
30	0	0	0	0	0	0	0	0
60	3.9	3.2	0	0	0	0	0	0
70	4.8	2.8	0	0	3.2	3.0	3.2	3.0
100	0	0	0.71	0.53	**2.6**	**0.98**	**2.6**	**0.98**
150	0	0	2.2	1.0	**0.36**	**0.11**	**0.36**	**0.11**
260	0	0	**3.8**	**1.3**	**0.36**	**0.16**	**2.1**	**0.74**
500	**2.5**	**0.98**	0	0	5.0	2.2	5.0	2.2
1000	0	0	0.74	0.7	0	0	0.74	0.7
PS2								
120	0	0	1.2	0.86	0	0	1.2	0.86
150	0	0	0	0	2.9	2.3	2.9	2.3
200	**7.2**	**2.5**	**1.6**	**0.46**	0	0	**1.6**	**0.46**
250	3.3	2.0	**4.3**	**1.1**	**4.1**	**1.2**	**4.2**	**1.2**
300	**1.6**	**0.58**	0	0	0	0	0	0
500	0	0	0	0	0.19	0.11	0.19	0.11
850	0	0	**4.5**	**1.4**	0	0	**4.5**	**1.4**
PS3								
16	0.8	0.53	0	0	0.52	0.41	0.52	0.41
25	**1.2**	**0.33**	0	0	**1.0**	**0.35**	**1.0**	**0.35**
35	0	0	0	0	0.53	0.27	0.53	0.27
45	0	0	0.24	0.21	0	0	0.24	0.21
60	0.33	0.28	**1.2**	**0.32**	**0.89**	**0.29**	**1.1**	**0.31**
70	0.7	0.33	**0.83**	**0.29**	**1.0**	**0.18**	**0.93**	**0.23**
100	0	0	**1.7**	**0.31**	**1.3**	**0.4**	**1.5**	**0.35**
160	1.9	0.89	**0.69**	**0.21**	**2.4**	**0.8**	**1.5**	**0.5**
250	0	0	**1.2**	**0.35**	0.94	0.71	**1.2**	**0.35**
800	0.47	0.33	**0.58**	**0.16**	0.34	0.26	**0.58**	**0.16**

Supplementary Table S3: Comparison of anammox rates calculated from $^{15}NH_4^+$ and $^{15}NO_2^-$ and denitrification rates from SR1805 cruise. Rates in bold are significantly different from zero. The consensus anammox rate was determined by (1) averaging the rates from the two tracers if both tracers returned a significant positive rate or (2) taking the rate from the tracer that returned a significant rate if the other tracer returned an insignificant rate or (3) taking the rate from the tracer that returned an insignificant but positive rate with error bars above zero if the other tracer returned a rate of zero.

Regression	Slope	Error	R^2	P value	Line type	Color
Shallow boundary – all data	0.56	0.059	0.55	1.4e-14	Solid	Orange
ODZ core – all data	0.45	0.053	0.54	9.5e-12	Solid	Teal
Shallow boundary – 2018 only	0.29	0.10	0.16	0.009	Dashed	Orange
ODZ core – 2018 only	0.35	0.038	0.79	2.5e-9	Dashed	Teal
Shallow boundary – 2012-13 only	0.64	0.073	0.69	3.1e-10	Dotted	Orange
ODZ core – 2012-13 only	1.1	0.13	0.68	2.3e-10	Dotted	Teal

Supplementary Table S4: Regression statistics for Fig. 9A (plot of denitrification vs. anammox rates).

Station	Depth (m)	NH$_4^+$ oxidation	Maximum N loss from NH$_4^+$ oxidation	Anammox	Denitrification	Total N loss	Percent N loss due to NH$_4^+$ oxidation	O$_2$
PS1	30	**0.0010**	0.0005	0.00	0.00	0.00	100	199.2
PS1	60	**0.8392**	0.4196	0.00	3.9	3.9	10.7	108.7
PS1	70	**1.0803**	0.5402	3.2	4.8	8.0	6.7	21.9
PS1	90	**0.2605**	0.1302	0.0	0.0	0.0	100	0.2
PS1	100	**0.3070**	0.1535	**2.6**	0.0	2.6	5.9	0.5
PS1	110	**0.0280**	0.0140	0.00	0.00	0.00	100	-0.1
PS1	150	**0.0014**	0.0007	**0.36**	0.00	0.36	0.2	0.4
PS1	260	**0.0005**	0.0003	**2.1**	0.0	2.1	0.0	2.9
PS1	500	**0.0002**	0.0001	5.0	**2.5**	7.6	0.0	-0.1
PS1	1000	**0.0002**	0.0001	0.7	0.0	0.7	0.0	30.1
PS2	60	**0.0293**	0.0146	0.0	0.0	0.0	100	174.5
PS2	75	**2.7476**	1.3738	0.0	0.0	0.0	100	47.0
PS2	95	**0.9789**	0.4894	0.0	0.0	0.0	100	3.2
PS2	120	**0.0093**	0.0046	1.2	0.0	1.2	0.4	-0.1
PS2	150	**0.0024**	0.0012	2.9	0.0	2.9	0.0	-0.1
PS2	200	**0.0025**	0.0012	**1.6**	**7.2**	8.7	0.0	0.0
PS2	250	0.0	0.0	**4.2**	3.3	7.5	0.0	1.2
PS2	300	**0.0**	0.0	0.00	**1.6**	1.6	0.0	-0.2
PS2	500	**0.0005**	0.0003	0.19	0.00	0.19	0.1	0.1
PS2	850	0.0	0.0	**4.5**	0.0	4.5	0.0	1.5
PS3	16	0.0	0.0	0.52	0.80	1.3	0.0	90.2
PS3	25	**11.7272**	5.8636	**1.0**	**1.2**	2.2	262	27.7
PS3	35	**6.3850**	3.1925	0.53	0.00	0.53	601	1.9
PS3	45	0.0	0.0	0.24	0.00	0.24	0.0	-0.2

Station	Depth (m)	NH$_4^+$ oxidation	Maximum N loss from NH$_4^+$ oxidation	Anammox	Denitrification	Total N loss	Percent N loss due to NH$_4^+$ oxidation	O$_2$
PS3	60	**0.1832**	0.0916	**1.1**	0.33	1.4	6.6	-0.3
PS3	70	0.00	0.0	**0.93**	0.70	1.6	0.0	0.0
PS3	100	**0.0294**	0.0147	**1.5**	0.0	1.5	1.0	0.1
PS3	160	**0.0061**	0.0031	**1.5**	1.9	3.4	0.1	0.0
PS3	250	0.0000	0.0000	**1.2**	0.0	1.2	0.0	0.0
PS3	800	**0.0345**	0.0173	**0.58**	0.47	1.1	1.6	0.3

Supplementary Table S5: N loss due to NH$_4^+$ oxidation does not contribute a large fraction (> 10% of total N loss) of the total N loss except in oxic depths or depths where denitrification and anammox are low (< 1 nM N$_2$ d^{-1}). NH$_4^+$ oxidation rates and the maximum N loss from NH$_4^+$ oxidation rates are in shown in nmol N d^{-1} and nmol N$_2$ d$^{-1,}$ respectively. Maximum N loss from NH$_4^+$ oxidation rates were calculated by unrealistically assuming that all ^{15}N-NO$_2^-$ produced in NH$_4^+$ oxidation was converted to N$_2$. Anammox, denitrification, and total N loss are shown in nmol N$_2$ d^{-1} and O$_2$ is shown in μM. Raw NH$_4^+$ oxidation, anammox, and denitrification rates that are significantly different from zero are shown in bold.
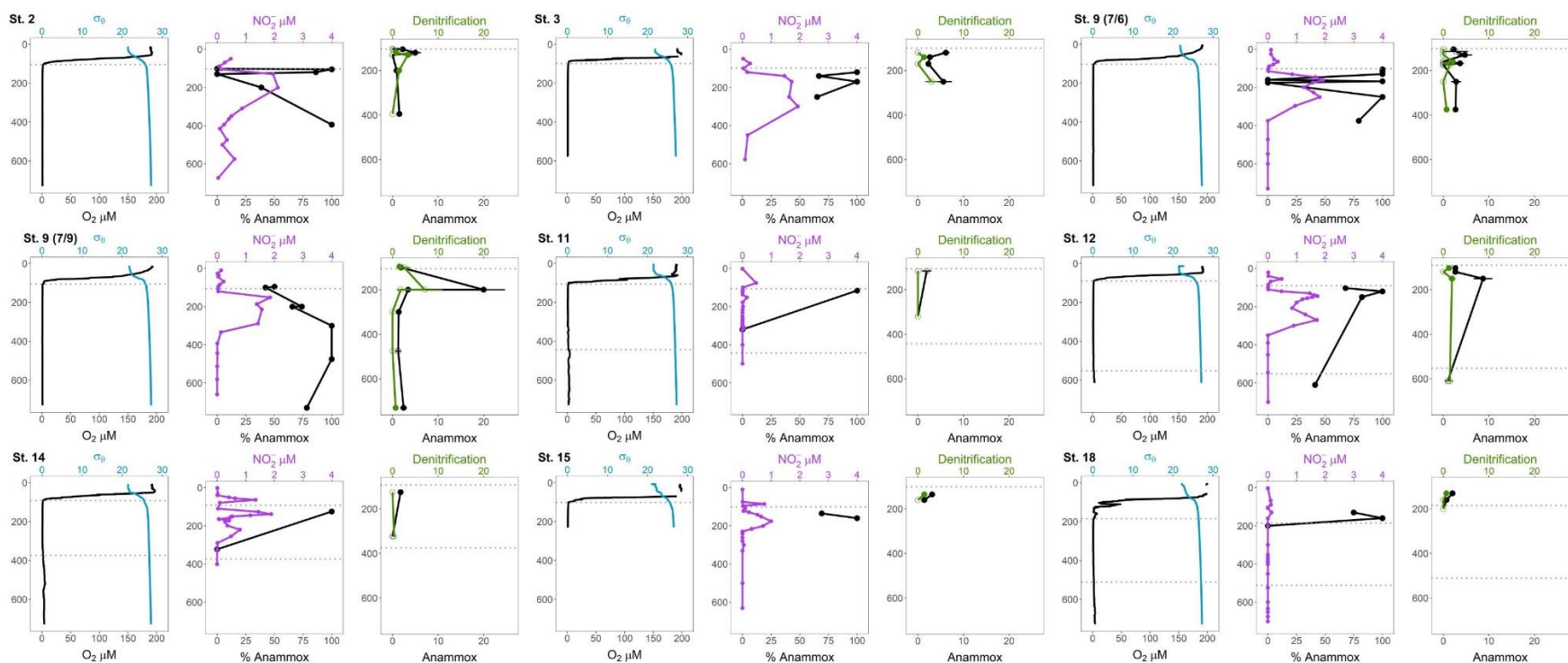
Figure S1: Depth profiles of biogeochemical parameters and N loss rate measurements from cruise FK180624. Measurements were conducted at eight stations along a gradient from waters (St. 2 and 3) similar to OMZ station PS2 (SR1805 cruise) to stations near the border of the OMZ region (St. 15 and 18) (Fig. 1). Station 9 was sampled multiple times for N loss measurements, once on 7/6/2018 and once on 7/9/2018. For each station, O_2 (μM) (black) and potential density (kg m^{-3}) (cyan) are shown in the first panel, NO_2^- (μM) (purple) and percent anammox values (black) are shown in the second panel, and anammox (black) and denitrification rates (green) (nM N$_2$ d^{-1}) are shown in the third panel. Grey dotted lines indicate the upper and lower boundaries of the deoxygenated ODZ region at the time of sampling. The bottom boundary was below the edge of the plot in stations 2, 3, and 9 while the CTD did not sample deeply enough to measure this feature for station 15. In the N loss plots, filled circles indicate rates significantly different from zero, while open circles are insignificant rates. Error bars indicate the standard error of the regression.

12
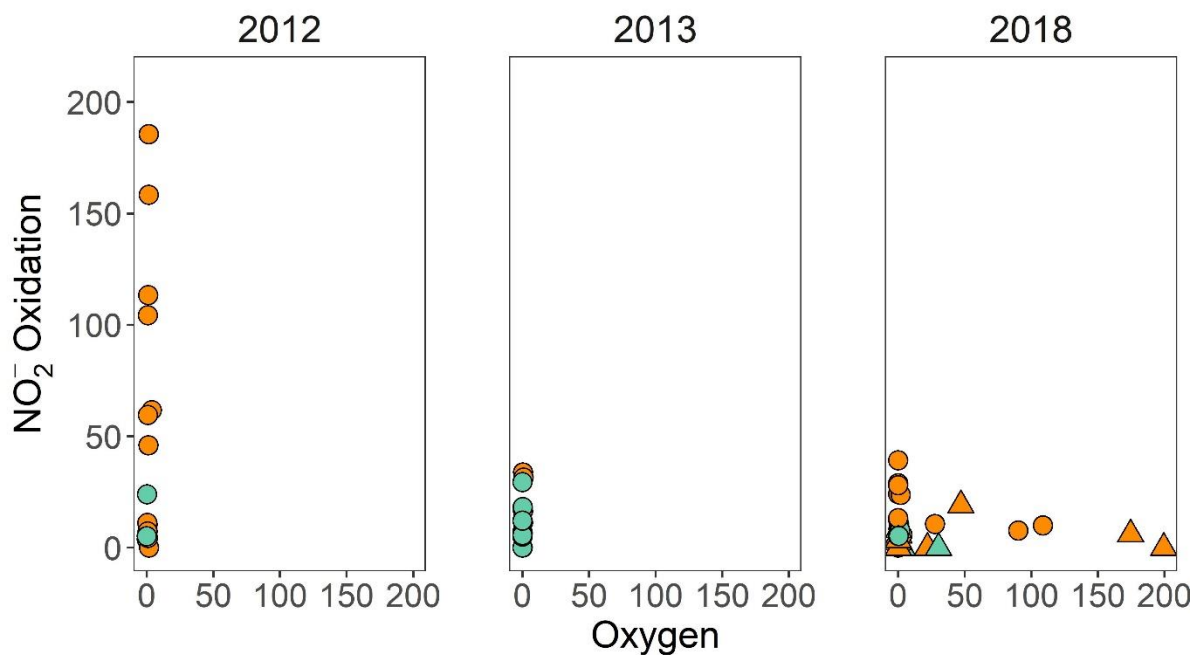
Figure S2: NO$_2^-$ oxidation rates (nM N d^{-1}) from the TN278, and NBP1305, and SR1805 cruises vs. O$_2$ concentration (μM) from the shipboard CTD sensors. O$_2$ concentrations were normalized across cruises. Rates that are significantly different from zero as assessed via a student T-test (p value < 0.05) are displayed as filled circles, while insignificant rates are displayed as triangles. Rates measured in shallow boundary waters are colored orange while rates from the ODZ core and below are colored teal. 2012 and 2013 data are republished (Babbin et al., 2020).
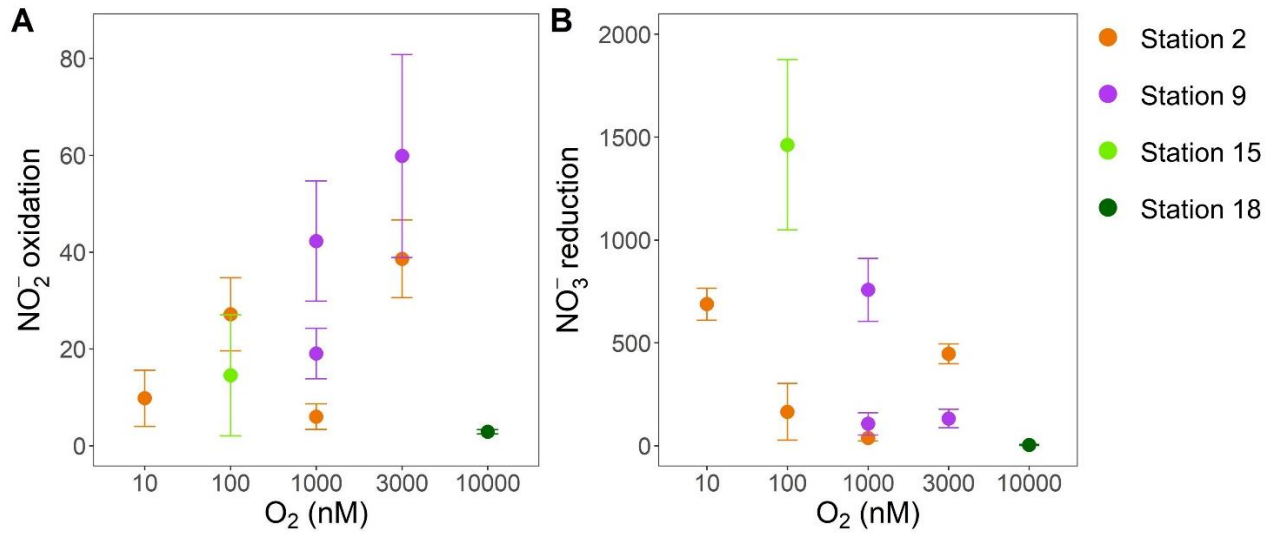
Figure S3: O_2 manipulation experiments from the FK180624 cruise in summer 2018. NO_2^- oxidation **(A)** and NO_3^- reduction **(B)** (nM N d^{-1}) measured across an O_2 gradient from 10 to 10000 nM. Station 2 (dark orange) is closest to shore and represents a similar region to station PS2 from cruise SR1805 in spring 2018. Station 9 (purple) is an intermediate environment between station 2 and stations 15 (light green) and 18 (dark green) which are farther offshore and represent the boundaries of the OMZ region (Fig. 1). Error bars represent the standard error of the regression.
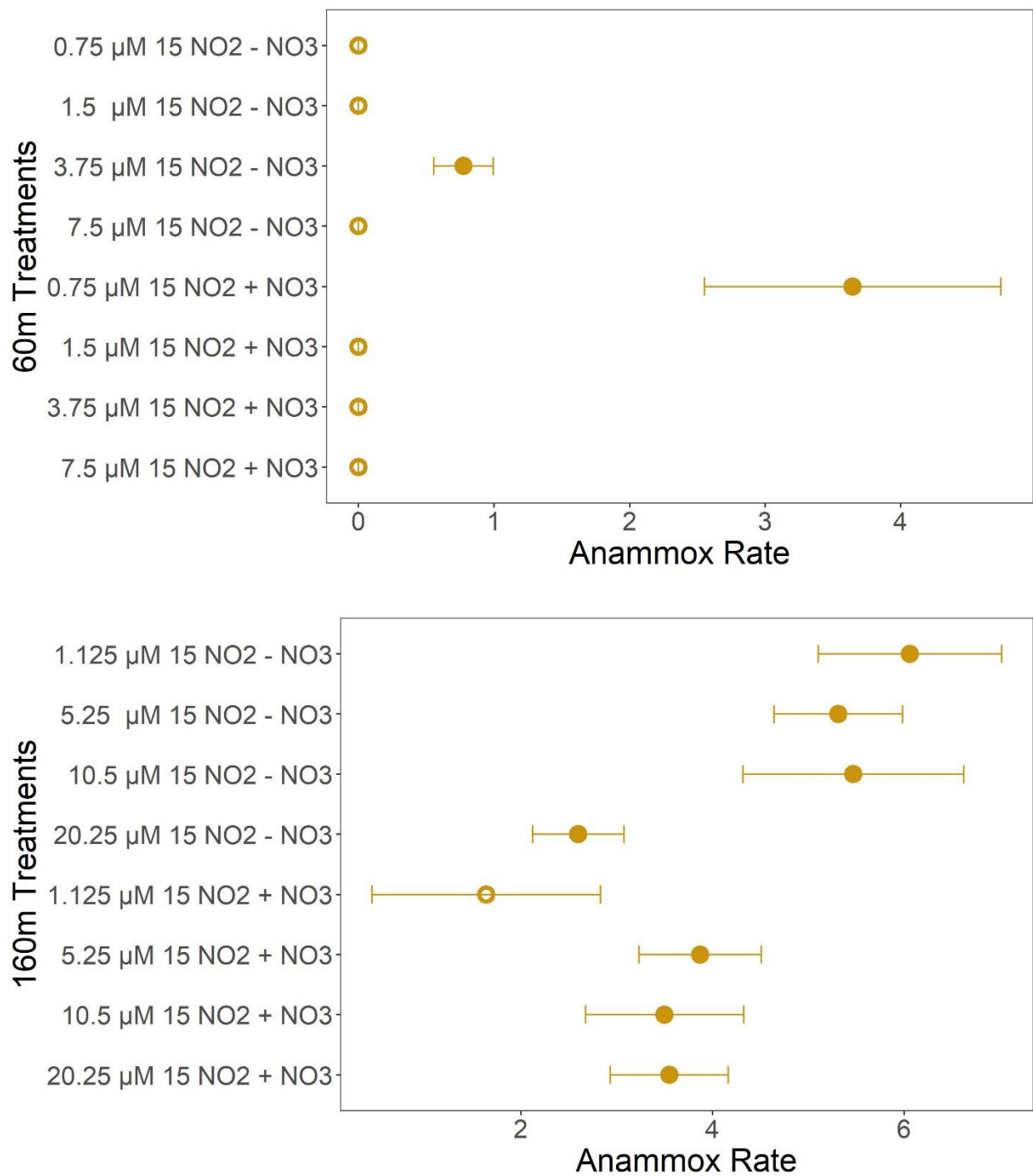
Figure S4: Anammox rates (nM d^{-1}) used to calculate the unexplained NO$_2^-$ oxidation rate in Fig. 5. Filled circles indicate significant rates while open circles indicate rates that are not significantly different from zero. Error bars are the standard error of the regression.
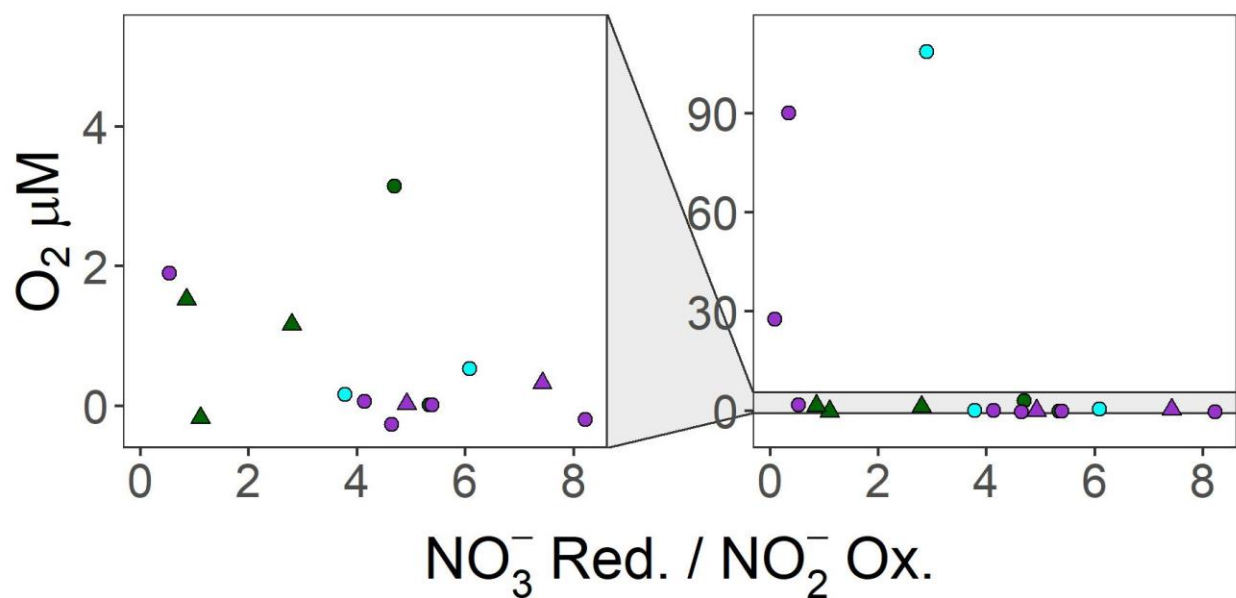
Figure S5: Oxygen does not differentially regulate NO_3^- reduction and NO_2^- oxidation. O_2 (µM) plotted against the ratio between the NO_3^- reduction rate and NO_2^- oxidation rate for all SR1805 depths with significant NO_2^- oxidation rates. Triangles indicate samples from the ODZ core or below ($\sigma_\theta > 26.4$) and circles depict samples from shallow boundary waters ($\sigma_\theta < 26.4$). Colors indicate station: purple (PS3), green (PS2), cyan (PS1).
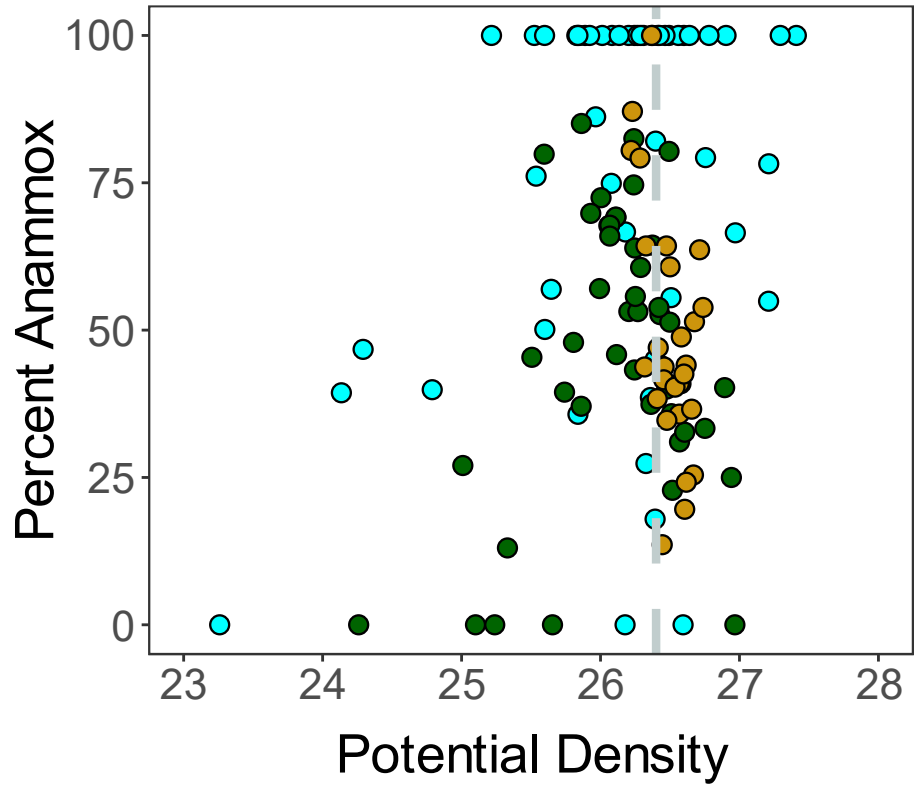
Figure S6: Percent anammox plotted against potential density for all cruises. Data from TN278 (ETNP 2012) is shown in green, NBP1305 (ETSP 2013) is shown in gold, and both 2018 cruises (SR1805 and FK180624) in cyan. The grey dashed line differentiates shallow boundary waters ($\sigma_\theta < 26.4$) and waters from the ODZ core and below ($\sigma_\theta > 26.4$).
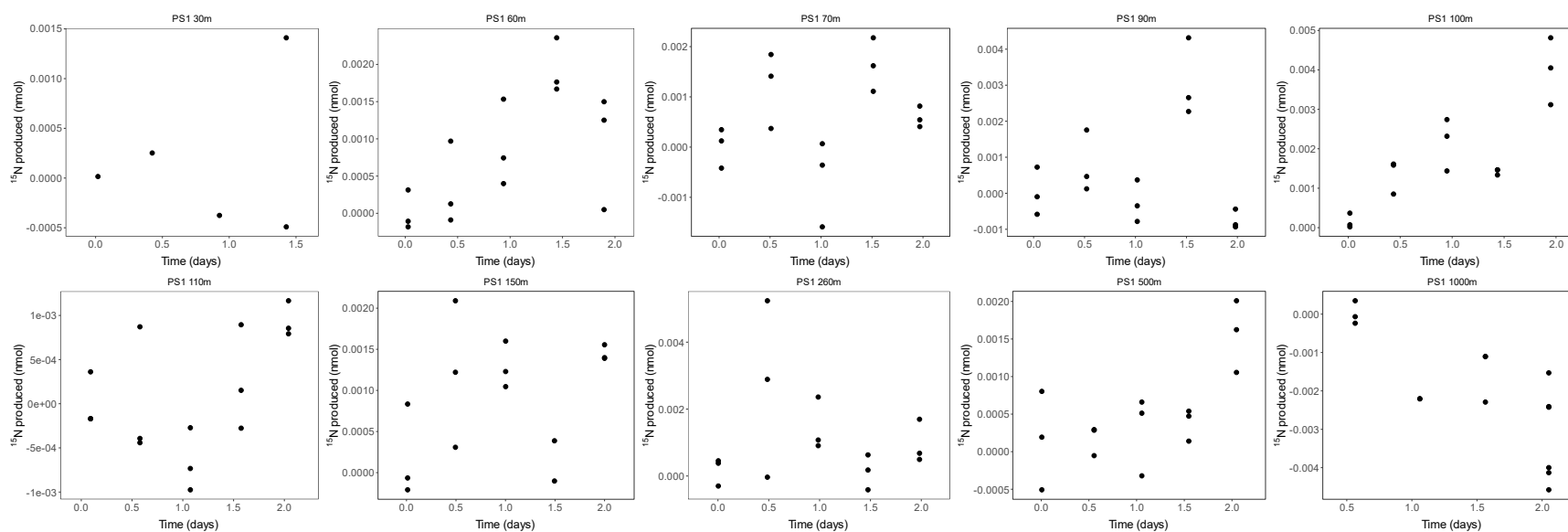
Figure S7: Time-courses from SR1805 NO_2^- oxidation depth profile experiments. All depths from station PS1 are shown. Top row, from left to right: 30, 60, 70, 90, 100 m, bottom row from left to right: 110, 150, 260, 500, 1000m. The y-axis depicts ^{15}N produced in nmol N while the x axis shows time in days. Complete time-courses are shown. For each depth, the best regression from $t_0 - t_2$, $t_0 - t_3$, or $t_0 - t_4$, was used to calculate the final rate plotted in Fig. 2.
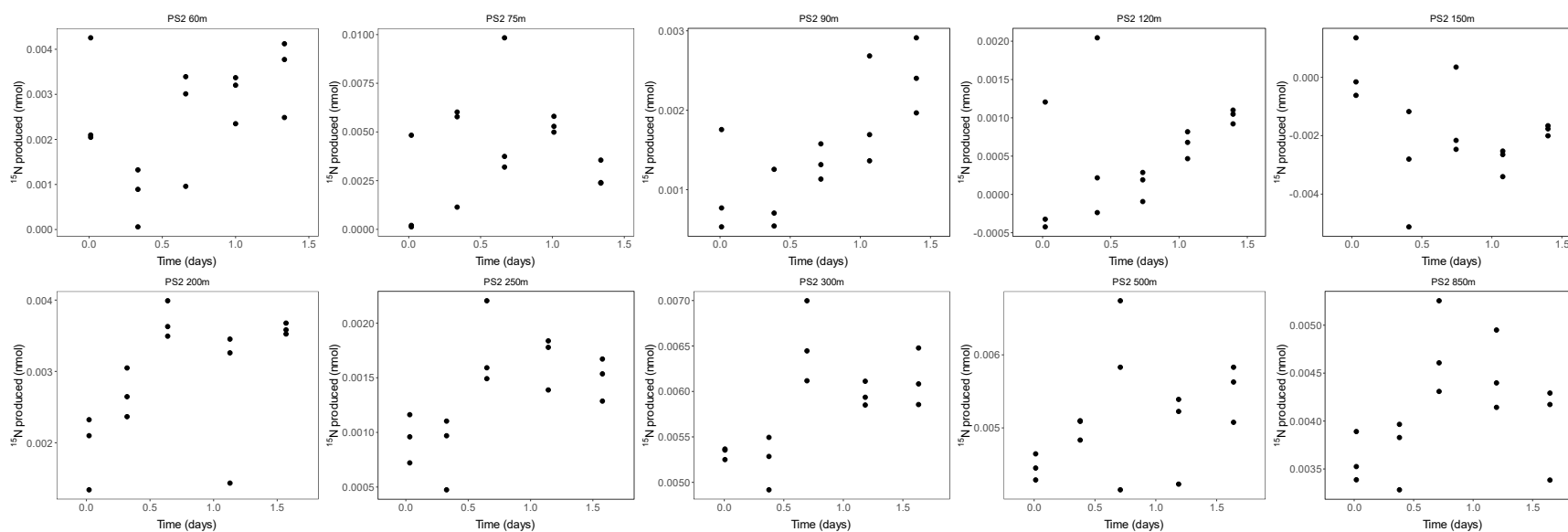
Figure S8: Time-courses from SR1805 NO_2^- oxidation depth profile experiments. All depths from station PS2 are shown. Top row from left to right: 60, 75, 90, 120, 150 m, bottom row from left to right: 200, 250, 300, 500, 850m. The y-axis depicts ^{15}N produced in nmol N while the x axis shows time in days. Complete time-courses are shown. For each depth, the best regression from $t_0 - t_2$, $t_0 - t_3$, or $t_0 - t_4$, was used to calculate the final rate plotted in Fig. 2.
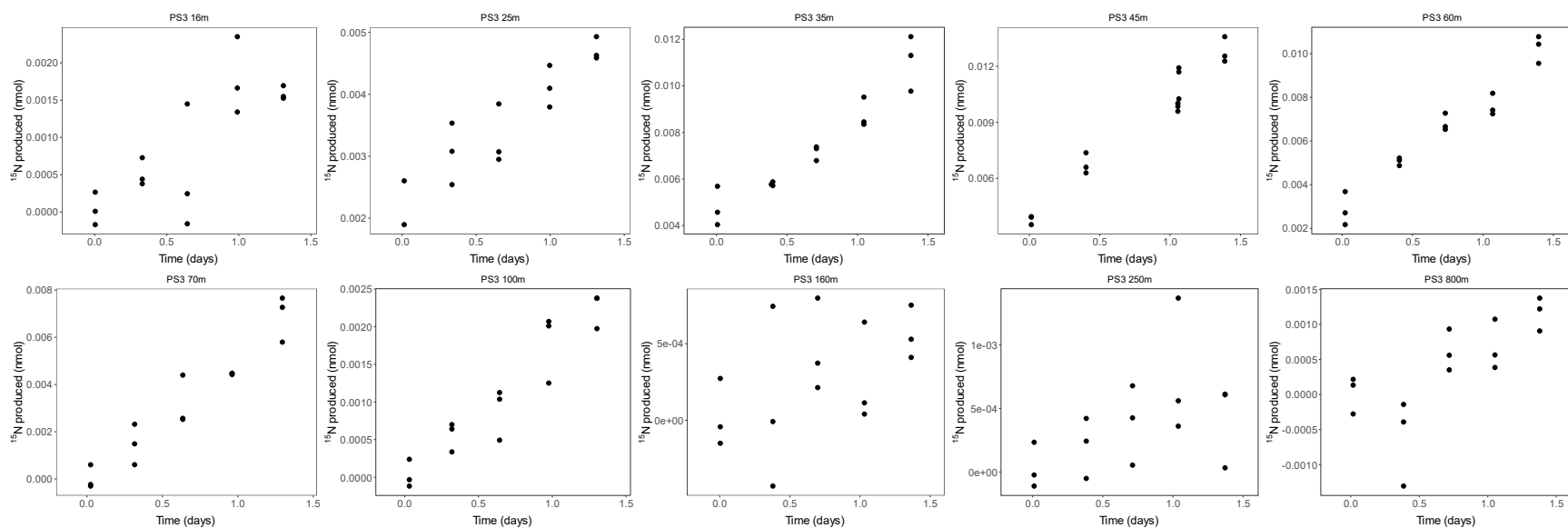
Figure S9: Time-courses from SR1805 NO_2^- oxidation depth profile experiments. All depths from station PS3 are shown. Top row from left to right: 16, 25, 35, 45, 60, bottom row from left to right: 70, 100, 160, 250, 800m. The y-axis depicts ^{15}N produced in nmol N while the x axis shows time in days. Complete time-courses are shown. For each depth, the best regression from $t_0 - t_2$, $t_0 - t_3$, or $t_0 - t_4$, was used to calculate the final rate plotted in Fig. 2.